RESEARCH ARTICLE

# Corrosion Inhibition of the Annealed 18 Ni 250 Grade Maraging Steel in 0.67 M Phosphoric Acid by 3,4-Dimethoxybenzaldehydethiosemicarbazone

*Chemical Sciences Journal, Vol. 2012: CSJ-69*

# Corrosion Inhibition of the Annealed 18 Ni 250 Grade Maraging Steel in 0.67 M Phosphoric Acid by 3,4-Dimethoxybenzaldehydethiosemicarbazone

**T Poornima[1]*, J Nayak[2], AN Shetty[3]**

[1]Department of Science and Humanities, PESIT, Bangalore, Karnataka, India.

[2]Department of Metallurgy and Materials Engineering; [3]Department of Chemistry; National Institute of Technology Karnataka, Surathkal, Srinivasnagar, Karnataka, India.

***Correspondence to:** Thombathu Poornima, poornimashettyt@gmail.com

**Accepted: Aug 27, 2012; Published: Sep 21, 2012**

**Abstract**

18 Ni 250 grade maraging steel is a potential high strength steel for advanced technologies such as aerospace, nuclear, and sporting goods. The corrosion inhibition of the aged 18 Ni 250 grade maraging steel in 0.67 M phosphoric acid by 3,4 dimethoxybenzaldehydethiosemicarbazone (DMBTSC) has been investigated by means of potentiodynamic polarization and electrochemical impedance spectroscopy (EIS) techniques. The effect of concentration of inhibitor and solution temperature on inhibition efficiency of the inhibitor was studied. DMBTSC inhibits corrosion even at very low concentration. Polarisation curves indicate mixed type inhibition behavior affecting both cathodic and anodic corrosion currents. The mechanism of inhibition was discussed on the basis of an adsorption isotherm, as well as calculated thermodynamic parameters. Adsorption of DMBTSC on the annealed maraging steel surface is in agreement with the Langmuir adsorption isotherm model, and the calculated Gibb's free energy values confirm the spontaneous adsorption.

**Keywords:** Maraging steel; polarisation; charge transfer resistance; adsorption.

## 1. Introduction

Corrosion of structural elements is a major issue for any industry because of the chemical environment of chemical processing. Inhibition is one of the most important applications in corrosion protection. Inhibitors protect the metal by adsorbing onto the surface and retard metal corrosion in aggressive environment. Selecting the appropriate inhibitor for specific environment and metal is of great importance, since the inhibitor which protects one particular metal may accelerate the corrosion of another. Maraging steels are special class of ultra high strength steels that differ from conventional steels in that they are hardened by a metallurgical reaction that does not involve carbon [1]. They derive high strength from age hardening of low carbon, Fe-Ni martensitic matrix [2]. Recently, the needs of high reliable substances of high strength and high ductility are gradually increased with the development of aerospace industry. The characteristics of this grey and white steel are high ductility, formability, high corrosion resistance, high temperature strength, ease of fabrication, weld ability and maintenance of an invariable size even after heat treatment [3]. According to available literature, atmospheric exposure of 18 Ni maraging steel leads to corrosion in a uniform manner and become completely rust covered [4]. Pit depths tend to be shallower than high strength steels [5]. Maraging steels are found to be less susceptible to hydrogen embrittlement than common high strength steels owing to significantly low diffusion of hydrogen in them [6]. Several technical papers covering alloy design, material processing, thermo-mechanical treatments, welding, strengthening mechanisms, etc., have been published [7]. These steels have emerged as alternative materials to conventional quenched and tempered steels for advanced technologies such as aerospace, nuclear and gas turbine applications. They frequently come in contact with acids during cleaning, pickling, descaling, acidizing, etc. Materials used in acid environment should have good corrosion resistance. Thiosemicarbazones and their derivatives have continued to be subject of extensive investigation in chemistry and biology owing to their broad spectrum of anti-tumor [8], antimalarial [9] and many other applications including corrosion inhibition of metals [10]. The inhibiting action of thiosemicarbazone derivatives has been mainly attributed to adsorption of thiocarbonyl group on the surface of metal. These compounds can be adsorbed on metal surface through lone pairs of electrons present on nitrogen or sulphur atoms and also through pi electrons present in these molecules

[11]. But, very less literature seems to be available which reveal corrosion behavior of 18 Ni 250 grade maraging steel in acid medium except our previous work [12]. So it is intended to study the corrosion inhibition of annealed 18 Ni 250 grade maraging steel in 0.67 M phosphoric acid medium using DMBTSC inhibitor.

## 2. Methods

### 2.1. Material

The maraging steel samples (M 250 grade) in annealed condition were taken from plates which were subjected to solution annealing treatment at 815 ± 5 $^{o}$C for 1 hour followed by air cooling. Percentage composition of 18 Ni 250 grade annealed maraging steel samples is given in Table 1. Cylindrical test coupons were cut from the plate and sealed with epoxy resin in such a way that, the area exposed to the medium is 0.503 cm$^2$.

**Table 1:** Composition of the annealed maraging steel specimen.

| Element | Composition | Element | Composition |
|---|---|---|---|
| C | 0.015 % | Ti | 0.3-0.6 % |
| Ni | 17-19 % | Al | 0.005-0.15 % |
| Mo | 4.6-5.2 % | Mn | 0.1 % |
| Co | 7-8.5 % | P | 0.01 % |
| Si | 0.1 % | S | 0.01 % |
| O | 30 ppm | N | 30 ppm |
| H | 2 ppm | Fe | Balance |

These coupons were polished as per standard metallographic practice, belt grinding followed by polishing on emery papers, finally on polishing wheel using legated alumina to obtain mirror finish, degreased with acetone, washed with double distilled water and dried before immersing in the corrosion medium. The inhibitor DMBTSC was synthesized in one step reaction of 3,4-dimethoxybenzaldehyde with thiosemicarbazide [9].

### 2.2. Medium

Standard solution of phosphoric acid having concentration 0.67 M was prepared by diluting analar grade 88% phosphoric acid by using double distilled water. The solutions of inhibitor with 5 ppm, 10 ppm, 20 ppm, 50 ppm concentration were prepared in 0.67 M phosphoric acid. Experiments were carried out using calibrated thermostat at temperatures 303 K, 308 K, 313 K, 318 K, 323 K (±0.5 K).

### 2.3. Electrochemical measurement

#### 2.3.1. Tafel polarisation studies

Electrochemical measurements were carried out by using an electrochemical work station, Auto Lab 30, Metrhom. Tafel plot measurements were carried out using conventional three electrode Pyrex glass cell with platinum counter electrode and saturated calomel electrode as reference electrode. Finely polished annealed maraging steel specimen of 0.503 cm$^2$ surface area was exposed to corrosion medium of 0.67 M phosphoric acid containing different concentrations of inhibitor at different temperatures (303 K to 323 K). The potentiodynamic current-potential curves were recorded by polarising the specimen to -250 mV cathodically and +250 mV anodically with respect to open circuit potential (OCP) at scan rate of 0.01 V/s. The electrode potential is plotted against the logarithm of applied current. The Tafel region is extrapolated to obtain corrosion potential and corrosion current density. The corrosion rate is calculated using equation 1.

$$\text{Corrosion rate (mm/y)} = \frac{3272(\text{E.W})I_{corr}}{D} \quad (1)$$

where 3272 is a constant that defines the unit of corrosion rate, $I_{corr}$ = corrosion current density in A/cm$^2$, D = density of the corroding material, 8.23 g/cm$^3$, E.W= 29.2, equivalent weight of corroding material (atomic weight/oxidation number) [13].

**2.3.2. Electrochemical impedance spectroscopy (EIS)**

EIS, which gives early information about the electrochemical processes, at the metal solution interface, has been used in many reports on the corrosion studies [14]. The corrosion inhibition behavior of the specimen was also obtained from EIS technique. In EIS technique a small amplitude AC signal of 10mV and frequency spectrum from 100,000 Hz to 0.01 Hz was impressed and impedance data are analyzed using Nyquist plots. The charge transfer resistance, $R_{ct}$ was extracted from the diameter of the semicircle in Nyquist plot.

## 3. Results and Discussion

### 3.1. Tafel polarization measurement

The corrosion inhibition of annealed samples of maraging steel specimen was investigated in 0.67 M phosphoric acid containing various concentration of DMBTSC inhibitor at different temperatures using Tafel polarization technique. The valuable potentiodynamic polarization parameters including corrosion potential ($E_{corr}$), corrosion current ($I_{corr}$), polarization resistance ($R_p$), anodic and cathodic slopes ($b_a$ and $b_c$), and corrosion rate (CR) were calculated from Tafel plots and are summarized in Table 2. These values predict substantial corrosion of annealed maraging steel in 0.67 M phosphoric acid. Figure 1 represents potentiodynamic polarization curves of annealed specimen in 0.67 M phosphoric acid containing different concentration of inhibitor under study at 30 $^0$C. The percentage inhibition efficiency (IE %) was calculated from expression (2).

$$IE\ \% = \frac{I_{corr} - I_{corr(inh)}}{I_{corr}} \quad (2)$$

where $I_{corr}$ and $I_{corr(inh)}$ are corrosion current densities in the absence and in presence of inhibitor respectively. The values of $I_{corr}$ decreases with increase in concentration of inhibitor. The decrease in $I_{corr}$ was observed even at low concentration of inhibitor. As can be seen in Figure 1, both cathodic and anodic corrosion reactions of the annealed maraging steel electrode were inhibited by the increase in DMBTSC concentration in 0.67 M phosphoric acid.

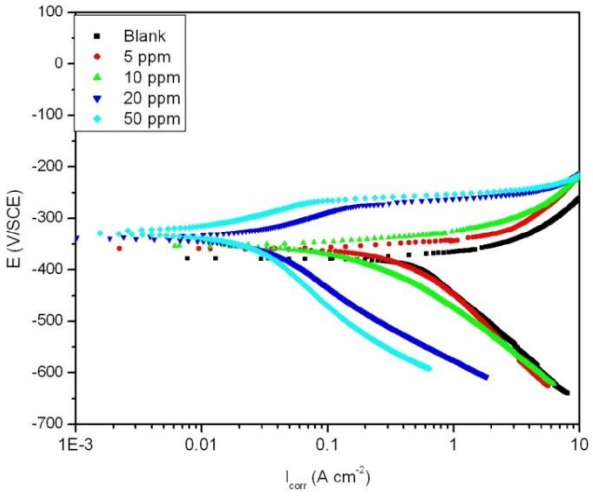


**Figure 1:** Tafel polarization curves of annealed maraging steel in 0.67 M phosphoric acid in the presence and absence of DMBTSC inhibitor at 303 K.

These results suggest that the addition of DMBTSC reduces anodic dissolution and also retards hydrogen evolution reaction. These observations indicated that this inhibitor exhibited cathodic and anodic inhibition effects. Therefore, this inhibitor can be classified as mixed type inhibitor.

**Table 2:** Results of Tafel polarization studies on annealed maraging steel in 0.67 M phosphoric acid containing various concentrations of DMBTSC.

| Temp. (K) | Conc. of inhibitor (ppm) | $E_{corr}$ (V) | $b_c$ (V/dec) | $b_a$ (V/dec) | $I_{corr} \times 10^{-4}$ (A $cm^{-2}$) | CR (mm/y) | IE % |
|---|---|---|---|---|---|---|---|
| 303 | 0 | -0.378 | 0.191 | 0.093 | 9.74 | 11.3 | |
| | 5 | -0.356 | 0.238 | 0.033 | 1.41 | 1.63 | 85.58 |
| | 10 | -0.348 | 0.202 | 0.028 | 1.13 | 1.31 | 88.41 |
| | 20 | -0.333 | 0.246 | 0.077 | 0.46 | 0.537 | 95.25 |
| | 50 | -0.324 | 0.198 | 0.117 | 0.25 | 0.285 | 97.48 |
| 308 | 0 | -0.38 | 0.175 | 0.099 | 11.03 | 12.8 | |
| | 5 | -0.347 | 0.203 | 0.035 | 1.89 | 2.19 | 82.89 |
| | 10 | -0.357 | 0.226 | 0.047 | 1.70 | 1.97 | 84.61 |
| | 20 | -0.314 | 0.246 | 0.045 | 0.61 | 0.704 | 94.50 |
| | 50 | -0.305 | 0.237 | 0.042 | 0.40 | 0.465 | 96.37 |
| 313 | 0 | -0.38 | 0.153 | 0.093 | 13.13 | 15.23 | |
| | 5 | -0.349 | 0.273 | 0.035 | 2.57 | 2.98 | 80.43 |
| | 10 | -0.367 | 0.226 | 0.047 | 2.18 | 2.53 | 83.39 |
| | 20 | -0.32 | 0.246 | 0.045 | 0.78 | 0.904 | 94.06 |
| | 50 | -0.355 | 0.137 | 0.042 | 0.56 | 0.65 | 95.73 |
| 318 | 0 | -0.38 | 0.126 | 0.073 | 14.77 | 17.13 | |
| | 5 | -0.361 | 0.218 | 0.053 | 3.63 | 4.21 | 75.42 |
| | 10 | -0.352 | 0.202 | 0.077 | 3.39 | 3.937 | 77.02 |
| | 20 | -0.344 | 0.246 | 0.112 | 2.16 | 2.503 | 85.39 |
| | 50 | -0.341 | 0.249 | 0.131 | 1.19 | 1.376 | 91.97 |
| 323 | 0 | -0.382 | 0.156 | 0.09 | 16.66 | 19.32 | |
| | 5 | -0.361 | 0.285 | 0.11 | 4.57 | 5.3 | 72.57 |
| | 10 | -0.352 | 0.276 | 0.077 | 4.26 | 4.94 | 74.43 |
| | 20 | -0.344 | 0.246 | 0.112 | 2.78 | 3.23 | 83.28 |
| | 50 | -0.341 | 0.272 | 0.091 | 2.31 | 2.68 | 86.13 |

The fact that $E_{corr}$ values shifted to positive side with increase in inhibitor concentration, suggests predominant anodic inhibition effect of DMBTSC. The parallel cathodic Tafel curves suggest that the hydrogen evolution is activation controlled and the reduction mechanism is not affected by the presence of the inhibitors. The values of $b_c$ changed slightly with increase in inhibitor concentration which indicates the influence of DMBTSC on the kinetics of hydrogen evolution. The shift in the anodic Tafel slope $b_a$ also suggests predominant anodic inhibition effect of DMBTSC, this may be due to the phosphate or inhibitor molecules adsorbed on the steel surface. For anodic polarization curves of specimen, it seems that the working electrode potential, higher than -250 mV/SCE, the presence of inhibitor does not change the current versus potential characteristics, this potential can be defined as desorption potential. The phenomenon may be due to the obvious metal dissolution, which leads to desorption of the inhibitor molecule from the electrode surface, in this case the desorption rate of the inhibitors is higher than its adsorption rate, so the corrosion current increases more obviously with rising potential [15].

### 3.1.1. Effect of temperature

The effect of temperature on the inhibited acid-metal reaction is highly complex because many changes occur on the metal surface, such as rapid etching and desorption of the inhibitor and the inhibitor itself, in some cases may undergo decomposition and/or rearrangement. However, it facilitates the calculation of many thermodynamic functions for the inhibition and/or the adsorption processes which contribute in determining the type of adsorption of the studied inhibitors. In the present study, with increase in solution temperature, corrosion potential ($E_{corr}$) and anodic Tafel slope ($b_a$), cathodic Tafel slope ($b_c$) values are not affected much. This indicates that increase in temperature does not change the mechanism of corrosion reaction. But, $I_{corr}$ and hence the corrosion rate of the specimen increases with increase in temperature for both blank and inhibited solutions. The inhibition efficiency decreases with increase in temperature which indicates desorption of indicator molecule. But,

this decrease is small at high concentration of inhibitor. The corrosion rate in acid solutions increases exponentially with increase in temperature because the hydrogen evolution over potential decreases with increase in temperature [16]. This result is in agreement with the observation reported by D. Jones that, in open system, the corrosion rate of iron increases with temperature up to 80 $^0$C [17]. It is evident from the values of corrosion rate given in Table 2 that the corrosion process exhibits Arrhenius type of dependence between corrosion rate and temperature. From the Arrhenius plots, the apparent activation energy ($E_a$) for the corrosion process in the presence and absence of inhibitor can be calculated using Arrhenius law equation (3) [18].

$$\ln (CR) = B - (E_a/RT) \quad (3)$$

where B is a constant which depends on the metal type and R is the universal gas constant. Corresponding Arrhenius plots are shown in Figure 2, from which $E_a$ has been evaluated.

The effect of chemically stable surface active inhibitors is to increase the energy of activation and to the diminution of the surface available for corrosion [19]. The value of activation energy ($E_a$) in 0.67 M phosphoric acid solution containing inhibitor was greater than that without inhibitor. The extent of increase is proportional to the inhibitor concentration, indicating that the energy barrier for the corrosion reaction increases with increase in DMBTSC concentration. The increase in apparent activation energy $E_a$ may be interpreted as physical adsorption [20]. Szauer and Brand [21] explained that the increase in activation energy can be attributed to an appreciable decrease in the adsorption of the inhibitor on the metal surface with increase in temperature and a corresponding increase in corrosion rate occurs due to the fact that greater area of metal is exposed to the acid environment.

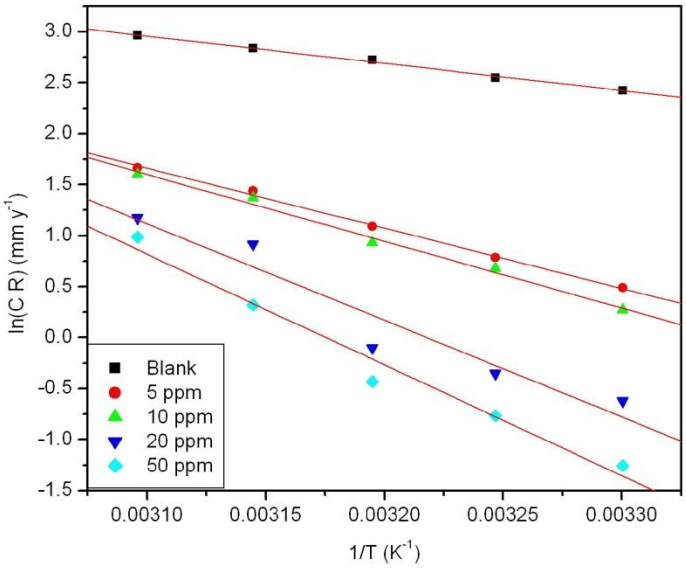


**Figure 2:** Arrhenius plots for the dissolution of annealed maraging steel in 0.67 M phosphoric acid containing different concentration of DMBTSC.

As it can be seen from Table 2, the corrosion rate of the specimen decreased with increase in concentration of inhibitor, hence it was clear that increment of $E_a$ was decisive factor affecting the corrosion rate of annealed maraging steel in 0.67 M phosphoric acid. Entropy and enthalpy of activation for the dissolution of alloy, ($\Delta H_a$&$\Delta S_a$) were calculated from transition state theory equation 4 [22].

$$CR = (RT/Nh) \exp (\Delta S_a/R) \exp (-\Delta H_a/RT) \quad (4)$$

where h is Plank's constant, N is Avagadro's number. A plot of ln(corrosion rate/T) vs 1/T gives straight line with slope = -ΔH/R and intercept = ln(R/Nh) + ΔS/R. The calculated values of $\Delta H_a$ and $\Delta S_a$ are given in Table 3. The plot of ln(corrosion rate/T) vs 1/T for annealed samples of maraging steel in various concentrations of inhibitor in 0.67 M phosphoric acid is shown in Figure 3. Thus, calculated values of activation parameters are given in Table 3. The entropy of activation in the presence of inhibitor is large and negative. This implies that the activated complex in

the rate determining step represents an association rather than dissociation step, meaning that a decrease in disordering takes place on going from reactants to activated complex [23].

**Table 3:** Activation parameters for the corrosion of annealed maraging steel in 0.67 M phosphoric acid containing different concentration of DMBTSC.

| Conc. of inhibitor (ppm) | $E_a$ (kJ mol$^{-1}$) | $\Delta H_a$ (kJ mol$^{-1}$) | $\Delta S_a$ (J mol$^{-1}$K$^{-1}$) |
|---|---|---|---|
| 0 | 22.2 | 19.6 | -160 |
| 5 | 49.1 | 46.4 | -87.9 |
| 10 | 54.5 | 51.9 | -71.4 |
| 20 | 78.9 | 76.3 | 0.03 |
| 50 | 90.4 | 87.8 | 33.6 |

The entropy of activation values are more for inhibited solutions than that for the uninhibited solutions. This suggested that an increase in randomness occurred on going from reactants to the activated complex. This might be the result of the adsorption of organic inhibitor molecules from the acidic solution which could be regarded as a quasi-substitution process between the organic compound in the aqueous phase and water molecules at electrode surface [24]. In this situation, the adsorption of organic inhibitor is accompanied by desorption of water molecules from the surface. Thus, the increasing entropy of activation was attributed to the increase in solvent entropy [25]. The positive ΔH values reflect the endothermic nature of dissolution process, meaning that dissolution of annealed maraging steel is difficult [26].

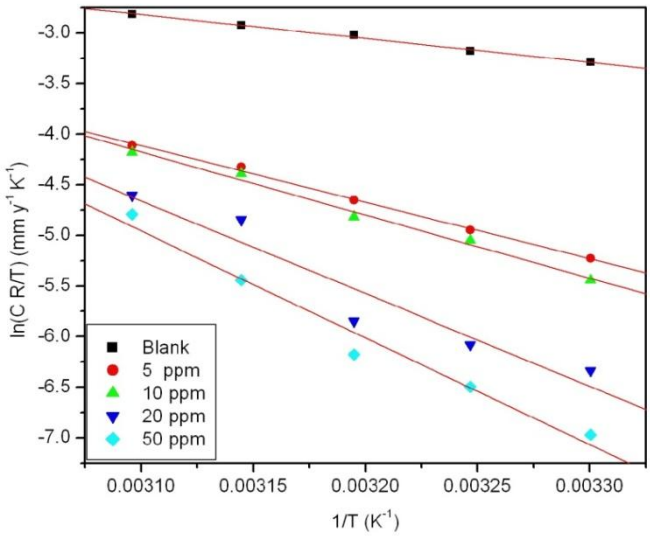


**Figure 3:** ln(corrosion rate)/T vs 1/T for dissolution of annealed maraging steel in 0.67 M phosphoric acid containing different concentration of DMBTSC.

### 3.2. Adsorption isotherm

Organic corrosion inhibitors are known to decrease metal dissolution via adsorption on the metal/corrodent interface to form a protective film which separates the metal surface from the corrosive medium. The adsorption route is usually regarded as a substitution process between the organic inhibitor in the aqueous solution [$Inh_{(sol)}$] and water molecules adsorbed at the metal surface [$H_2O_{(ads)}$] as follows [26].

$$Inh_{(sol)} + \chi\, H_2O_{(ads)} \leftrightarrow Inh_{(ads)} + \chi\, H_2O_{(sol)}$$

where χ represents the number of water molecules replaced by one molecule of adsorbed inhibitor. The adsorption bond strength is dependent on the composition of the metal, corrodent, inhibitor structure, concentration and orientation as well as temperature. Basic information on the interaction between the inhibitor

and alloy surface can be provided by adsorption isotherm. In order to obtain isotherm, the linear relation between surface coverage (θ) value and $C_{inh}$ must be found. Attempts were made to fit the θ values to various isotherms including Langmuir, Temkin, Frumkin and Flory-Huggins isotherms. By far the best fit is obtained with the modified Langmuir adsorption isotherm. The following equation (5) can be used,

$$\frac{C_{inh}}{\theta} = \frac{1}{K} + C_{inh} \quad (5)$$

where $C_{inh}$ is the concentration of inhibitor, K is the equilibrium constant for adsorption process, and θ is the degree of the surface coverage which is calculated using equation (6).

$$\theta = \frac{IE\%}{100} \quad (6)$$

where IE% is percentage inhibition efficiency as calculated using equation (2).

This model has also been used for other inhibitor systems [26]. The plots of $C_{inh}/\theta$ vs $C_{inh}$ yields a straight line with intercept 1/K as shown in Figure 4. The values of standard free energy of adsorption are related to K by the relation (7).

$$K = \frac{1}{55.5} e^{(-\frac{\Delta G^0_{ads}}{RT})} \quad (7)$$

where the value 55.5 is the concentration of water in solution in M (mol/L), R is the universal gas constant and T is absolute temperature [27, 28]. The thermodynamic data obtained from adsorption isotherm are depicted in Table 4. The correlation coefficient ($R^2$) was used to choose the isotherm that best fit experimental data. The linear regression coefficients are close to unity and the slopes of straight lines are nearly unity, suggesting that the adsorption of DMBTSC obeys Langmuir's adsorption isotherm and there is negligible interaction between the adsorbed molecules [29]. The high values of K for the studied inhibitor indicate strong adsorption of inhibitor on the alloy surface. Negative values of $\Delta G^0_{ads}$ are characteristic feature of strong spontaneous adsorption for the studied compounds, which also reflect the high values of inhibition. The negative $\Delta G_{ads}$ values calculated from equation (7) are consistent with the spontaneity of the adsorption process and the stability of the adsorbed layer on the carbon steel surface. Generally the energy values of -20 kJ/mol$^{-1}$ or less negative are associated with an electrostatic interaction between charged molecules and charged metal surface, physisorption, those of -40 kJ mol$^{-1}$ or more negative involve charge sharing or transfer from the inhibitor molecules to the metal surface to form a coordinate covalent bond, chemisorption [30].

The $\Delta G_{ads}$ values obtained for the studied inhibitor on the alloy surface in 0.67 M phosphoric acid are -40 to -43 kJ/mol, this indicates that the adsorption is not typical physisorption. The unshared electron pairs in the inhibitor molecule interact with d-orbitals of iron to provide a protective chemisorbed film. Similar conclusions were drawn by Machnikova *et al.* [27] and Singh *et al.* [31]. A plot of $\Delta G^0_{ads}$ versus T gave heat of adsorption $\Delta H^0_{ads}$ and the standard adsorption entropy $\Delta S^0_{ads}$ according to the thermodynamic equation (8),

$$\Delta G^0_{ads} = \Delta H^0_{ads} - T\Delta S^0_{ads} \quad (8)$$

The thermodynamic data obtained for DMBTSC using Langmuir adsorption isotherm are depicted in Table 4. The values of thermodynamic parameters for the adsorption of inhibitors can provide valuable information about the mechanism of corrosion inhibition. While an endothermic adsorption process ($\Delta H^0_{ads} > 0$) is attributed unequivocally to chemisorption [32], an exothermic adsorption process ($\Delta H^0_{ads} < 0$) may involve either physisorption or chemisorption or a mixture of both the processes.

In an exothermic process, physisorption is distinguished from chemisorption by considering the absolute value of adsorption enthalpy. Typically, the enthalpy of a physisorption process is lower than 41.86 KJ/mol, while that of a chemisorption process approaches 100 k J /mol [32]. In the presented case, the calculated absolute value of $\Delta H^0_{ads}$ is 84 kJ mol$^{-1}$, which is relatively high, approaching those typical of chemisorption [32]. The $\Delta S^0_{ads}$ values in the presence of DMBTSC is large and negative, meaning that an disordering takes place in going from reactants to the metal adsorbed species reaction complex [33]. This may be due to replacement of water molecules from the surface during adsorption of inhibitor molecules, resulting in a decrease in disordering [34].

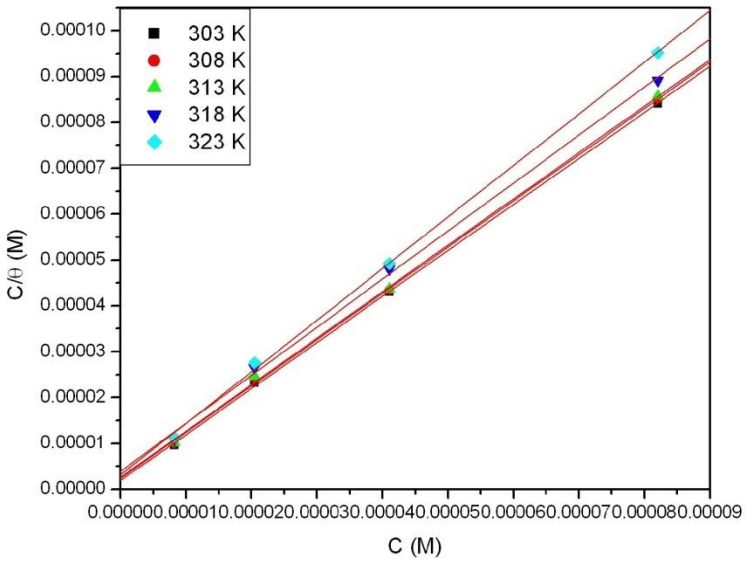


**Figure 4:** Fitting Langmuir adsorption isotherm of DMBTSC on annealed maraging steel in 0.67 M phosphoric acid at different temperatures.

**Table 4:** Thermodynamic parameters for the adsorption of DMBTSC on annealed maraging steel surface in 0.67 M phosphoric acid at different temperatures.

| Temp. (K) | K ($M^{-1}$) | $-\Delta G_{ads}$ (kJ $mol^{-1}$) | $R^2$ | $\Delta H_{ads}$ (kJ $mol^{-1}$) | $\Delta S_{ads}$ (J $mol^{-1}$ $K^{-1}$) |
|---|---|---|---|---|---|
| 303 | 521920 | 43.28 | 0.9999 | | |
| 308 | 420168 | 42.74 | 0.9942 | -84.69 | -146 |
| 313 | 362555 | 41.48 | 0.9992 | | |
| 318 | 255427 | 41.74 | 0.9942 | | |
| 323 | 117460 | 40.12 | 0.9985 | | |

### 3.3. Electrochemical impedance spectroscopy

The results of potentiodynamic polarization experiments were confirmed by impedance measurements, since EIS is a powerful technique in studying corrosion mechanism. In order to get more information about the corrosion inhibition of annealed maraging steel specimens in 0.67 M phosphoric acid containing DMBTSC, EIS measurements were carried out at different temperatures and they are displayed as Nyquist plots in the present study. The Nyquist plots obtained for annealed samples of maraging steel specimens in 0.67 M phosphoric acid with and without various concentrations of DMBTSC are as shown in Figure 5. From Figure 5 it is clear that the shapes of the impedance plots for inhibited electrodes are not substantially different from those of uninhibited electrodes. The presence of inhibitor increases the impedance but doesn't change other aspects of the behavior. These results support the results of polarization measurements that the inhibitor does not alter the electrochemical reactions responsible for corrosion. It inhibits corrosion primarily through its adsorption on the metal surface. The present study shows depressed capacitive loop at high frequency range (HF) whose diameter increases with increase in inhibitor concentration, followed by an inductive loop that is observed in low frequency (LF) region. The depressed capacitive loop with centre below real axis may be due to the contribution from surface roughness, distribution of active sites, adsorption of inhibitors and formation of porous layers as reported by others [35]. The impedance spectra for different Nyquist's plots were analyzed by fitting the experimental data to the equivalent circuit model as given in Figure 6 which has been used previously to model iron/acid interface [16]. The HF capacitive loop can be attributed to charge transfer reaction and time constant of the electric double layer [31].

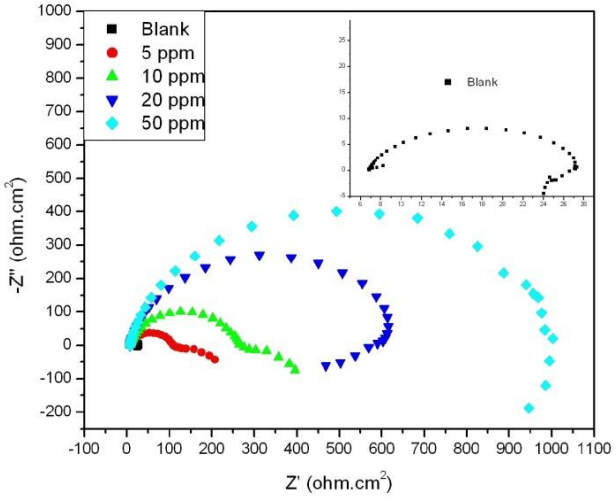


**Figure 5:** Nyquist plots for annealed maraging steel specimen in 0.67 M phosphoric acid with and without inhibitors.

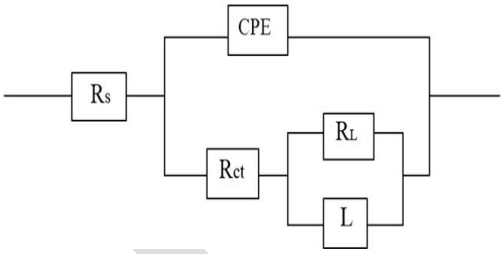


**Figure 6:** Equivalent circuit used to fit experimental EIS data for the corrosion of maraging steel specimen in phosphoric acid.

These are not perfect semicircles, because the Nyquist plots obtained in the real system represent a general behavior where the double layer at the metal solution interface does not behave as an ideal capacitor [36]. The LF inductive loop can be attributed to relaxation process obtained by adsorbed sulphate ions and protons. It may also be attributed to the redissolution of the passivated surface at low frequencies [37]. We have correlated the low frequency inductive loop in inhibitor free acid medium, with surface dissolution process. The low frequency inductive loop in inhibited acid solution might be attributed to the relaxation process obtained by adsorption of $H^+$ and phosphate on the electrode surface. It might also be attributed to the re-dissolution of the passivated surface at low frequencies.

The point of intersection between inductive loop and the real axis represents ($R_s$ + $R_{ct}$). $R_s$ represents solution resistance due to the ohmic resistances of corrosion product films and the solution enclosed between the working electrode and the reference electrode. $R_{ct}$ represents the charge transfer resistance whose value is a measure of electron transfer across the surface and is inversely proportional to corrosion rate [38]. The presence of L in the impedance spectra in the presence of inhibitor indicates that alloy is still dissolved by the direct charge transfer at the inhibitor adsorbed alloy surface [39].

The charge transfer resistance $R_{ct}$ and double layer capacitance $C_{dl}$ were determined by the analysis of Nyquist plot and their values are given in Table 5. The inhibition efficiency in different concentrations of DMBTSC was calculated from the charge transfer resistance according to equation,

$$IE\% = \left( \frac{R_{ct} - R^{0}_{ct}}{R_{ct}} \right) \times 100 \qquad (9)$$

where $R_{ct}$ and $R^0_{ct}$ represent the charge transfer resistance in the presence and absence of inhibitor. The values of $R_{ct}$ increase with increase in inhibitor concentration and the results indicate that charge transfer process mainly controls the corrosion process.

**Table 5:** EIS data of annealed maraging steel in 0.67 M acid in absence and presence of different concentrations of inhibitor DMBTSC.

| Temp. (K) | Conc. of inhibitor (ppm) | $R_{ct}$ (ohm.cm$^2$) | $C_{dl}$ (μF cm$^{-2}$) | %IE |
|---|---|---|---|---|
| 303 | 0 | 21.2 | 974 | |
| | 5 | 127 | 249 | 83.31 |
| | 10 | 265 | 189 | 92.0 |
| | 20 | 546 | 173 | 96.12 |
| | 50 | 1002 | 145 | 97.88 |
| 308 | 0 | 18.6 | 1060 | |
| | 5 | 95 | 354 | 80.42 |
| | 10 | 123 | 288 | 84.87 |
| | 20 | 349 | 250 | 94.67 |
| | 50 | 624 | 193 | 97.02 |
| 313 | 0 | 15.8 | 1342 | |
| | 5 | 56.8 | 370 | 72.18 |
| | 10 | 100 | 306 | 84.20 |
| | 20 | 259 | 284 | 93.89 |
| | 50 | 520 | 207 | 96.96 |
| 318 | 0 | 13.6 | 1431 | |
| | 5 | 42 | 362 | 67.62 |
| | 10 | 72 | 330 | 81.11 |
| | 20 | 210 | 298 | 93.53 |
| | 50 | 421 | 227 | 96.76 |
| 323 | 0 | 12.1 | 1610 | |
| | 5 | 38 | 404 | 68.16 |
| | 10 | 62 | 362 | 80.48 |
| | 20 | 178 | 328 | 93.20 |
| | 50 | 351 | 245 | 96.55 |

The value of $C_{dl}$ decreases due to adsorption of inhibitor molecules, which displaces water molecules originally adsorbed on the mild steel surface and decreases the active surface area. The values of double layer capacitance decreases with increase in inhibitor concentration indicating that inhibitor molecules function by adsorption at the metal/solution interface, leading to protective film on the steel surface, and then decreasing the extent of dissolution reaction.

### 3.4. Scanning electron microscope (SEM)

The scanning electron microscope images were recorded to establish the interaction of acid medium with the metal surface using JEOL JSM-6380LA analytical scanning electron microscope. The surface morphology of the aged samples was examined by SEM immediately after corrosion tests in phosphoric medium. The SEM image of corroded annealed sample in Figure 7(a) shows degradation of alloy. Figure 7(b) represents SEM image of annealed maraging steel after the corrosion tests in a medium of phosphoric acid containing DMBTSC, which clearly shows the adsorbed layer of inhibitor molecules on the alloy surface thus protecting the metal from corrosion.

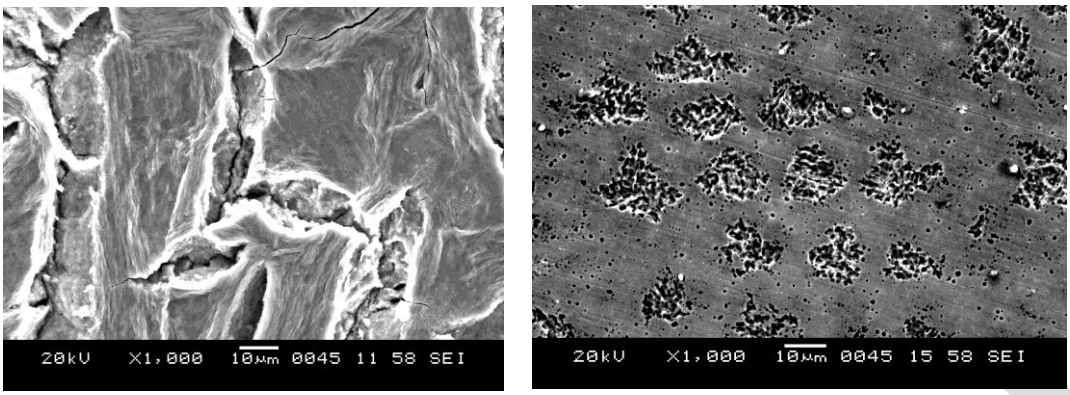


(a) (b)

**Figure 7:** SEM images of maraging steel (a) after immersion in 0.67 M phosphoric acid; (b) after immersion in 0.67 M phosphoric acid containing DMBTSC.

**4. Conclusion**

In this work, potentiodynamic polarization and electrochemical impedance methods are used to evaluate the ability of DMBTSC to inhibit corrosion of annealed maraging steel in 0.67 M phosphoric acid. The principal conclusions drawn are

1. The corrosion of annealed maraging steel in 0.67 M phosphoric acid is substantial.
2. The corrosion is significantly reduced by the addition of DMBTSC even at low concentration.
3. The inhibition efficiency increases with increase in inhibitor concentration.
4. The inhibition efficiency decreases with increase temperature.
5. DMBTSC acts as mixed type inhibitor, affecting both anodic and cathodic reactions with predominant anodic inhibition effect.
6. The adsorption of DMBTSC on annealed maraging steel surface obeys Langmuir's adsorption isotherm model.
7. The negative values of $\Delta G^0$ obtained from this study indicates that DMBTSC adsorbed spontaneously by both physisorption and chemisorption on the annealed maraging steel surface. The adsorption process is exothermic and accompanied by decrease in entropy.
8. SEM images revealed protection of alloy surface by DMBTSC in phosphoric acid medium.
9. The inhibition efficiency obtained from potentiodynamic polarization and EIS techniques are in reasonably good agreement.

**Competing Interests**

Authors do not have any competing interests.

**Authors' Contributions**

All authors have equally contributed to this research work.

**References**

1. Sastry KY, Narayanan R, Shamantha CR, Sunderason SS, Seshadri SK, Radhakrishnan VM, *et al.*, 2003. Stress corrosion cracking of maraging steel weldments. Materials Science and Technology, 19:375-381.
2. Rohrbach K, Schmidt M, 1990. Maraging Steels, ASM Handbook, 10th edn., Vol. 1, 796, American Chemical Society.
3. Lee DG, Jang KC, Kuk JM, Kim IS, 2005. The influence of niobium and aging treatment in the 18 % Ni maraging steel. Journal of Materials Processing Technology, 162-163:342-349.
4. Kirk WW, Covert RA, May TP, 1968. Corrosion behaviour of high-strength steels in marine environment, Metals Engineering Quarterly, 8:31-38.
5. Dean SW, Copson HR, 1965. Stress corrosion behaviour of maraging steel in natural environments. Corrosion, 21:95-103.
6. Rezek J, Klein IE, Yhalom J, 1997. Electrochemical properties of protective coatings on maraging steel. Corrosion Science, 39:385-397.
7. Sinha PP, 1982. Design and development of new variety of 250 grade stainless steel maraging steel. Trans IIM, 35:2.

8. Singh S, Athar F, Azam A, 2005. Synthesis, spectral studies and in vitro assessment for antiamoebic activity of new cyclooctadiene ruthenium(ii) complexes with 5-nitrothiophene-2-carboxaldehyde thiosemicarbazones. Bioorganic and Medicinal Chemistry Letters, 15:5424-5428.
9. de Oliveira RB, de Souza-Fagundes EM, Soares RPP, Andrade AA, Krettli AU, Zani CL, 2008. Synthesis and antimalarial activity of semicarbazone and thiosemicarbazone derivatives. European Journal of Medicinal Chemistry, 43:1984.
10. Arab ST, 2008. Inhibition of thiosemicarbazone and some of its p-substituted compounds on the corrosion of iron-base metallic glass alloy in 0.5 M $H_2SO_4$ at 30 $^{o}$C. Materials Research Bulletin, 43:510-521.
11. El-Shafei AA, Moussa MNH, El-Far AA, 2001. The corrosion inhibition character of thiosemicarbazide and its derivatives for C-steel in hydrochloric acid solution. Materials Chemistry and Physics, 70:175-180.
12. Poornima T, Nayak J, Shetty AN, 2010. Corrosion of aged and annealed 18 Ni 250 grade maraging steel in phosphoric acid medium. International Journal of Electrochemical Science, 5:56–71.
13. Saliyan VR, Adhikari AV, 2008. Quinolin-5-ylmethylene-3-{[8-(trifluoromethyl)quinolin-4-yl]thio}propanohydrazide as an effective inhibitor of mild steel corrosion in HCl solution. Corrosion Science, 50:55-61.
14. Battilana QM, Bonaldo L, Tortato T, 2008. Investigation of the inhibition effect of indole-3-carboxylic acid on the copper corrosion in 0.5 M $H_2SO_4$. Corrosion Science, 50:3467-3474.
15. Aksut AA, Lorenz WJ, Mansfeld F, 1982. The determination of corrosion rates by electrochemical d.c. and a.c. methods — II. Systems with discontinuous steady state polarization behavior. Corrosion Science, 22:611-619.
16. Popova A, Sokolova E, Raicheva S, Christov M, 2003. AC and DC study of the temperature effect on mild steel corrosion in acid media in the presence of benzimidazole derivatives. Corrosion Science, 45:33-58.
17. Speller FN, 1951. Corrosion Causes and Prevention, 3$^{rd}$ edition. McGraw Hill, 168.
18. Bouklah M, Hammouti B, Aounti A, Benhadda T, 2004. Thiophene derivatives as effective inhibitors for the corrosion of steel in 0.5 M $H_2SO_4$. Progress in Organic Coatings, 49:225-228.
19. Antropov L, 1967. A correlation between kinetics of corrosion and the mechanism of inhibition by organic compounds. Corrosion Science, 7:607-620.
20. Sherbini EFE, 1999. Effect of some ethoxylated fatty acids on the corrosion behaviour of mild steel in sulphuric acid solution. Materials Chemistry and Physics, 60:286-290.
21. Szauer T, Brand A, 1981. On the role of fatty acid in adsorption and corrosion inhibition of iron by amine—fatty acid salts in acidic solution. Electrochimica Acta, 26:1257-1260.
22. Abdel Rehim SS, Magdy AM, Ibrahim KF, 1999. 4-Aminoantipyrine as an inhibitor of mild steel corrosion in HCl solution. Journal of Applied Electrochemistry, 29:593-599.
23. Gomma MK, Wahdan MH, 1995. Schiff bases as corrosion inhibitors for aluminium in hydrochloric acid solution. Materials Chemistry and Physics, 39:209-213.
24. Sahin M, Bilgic S, Yilmaz H, 2002. The inhibition effects of some cyclic nitrogen compounds on the corrosion of the steel in NaCl mediums. Applied Surface Science, 195:1-7.
25. Ateya B, El-Anadouli BE, El-Nizamy FM, 1984. The adsorption of thiourea on mild steel. Corrosion Science, 24:509-515.
26. Mu GN, Li X, Li F, 2004. Synergistic inhibition between o-phenanthroline and chloride ion on cold rolled steel corrosion in phosphoric acid. Materials Chemistry and Physics, 86(1):59-68.
27. Machnikova E, Whitmire KH, Hackerman N, 2008. Corrosion inhibition of carbon steel in hydrochloric acid by furan derivatives. Electrochimica Acta, 53:6024-6032.
28. Kliskic M, Radosevic J, Gudic S, Katalinic V, 2000. Aqueous extract of *Rosmarinus officinalis* L. as inhibitor of Al–Mg alloy corrosion in chloride solution. Journal of Applied Electrochemistry, 30:823-830.
29. Fuchs-Godec R, 2006. The adsorption, CMC determination and corrosion inhibition of some *N*-alkyl quaternary ammonium salts on carbon steel surface in 2M $H_2SO_4$. Colloids and Surfaces A: Physicochemical and Engineering Aspects, 280:130-139.
30. Ehteshamzadeh M, Shahrabi T, Hosseini M, 2006. Innovation in acid pickling treatments of copper by characterizations of a new series of Schiff bases as corrosion inhibitors. Anti-Corrosion Methods and Materials, 53:296-302.
31. Singh AK, Quraishi MA, 2010. Effect of Cefazolin on the corrosion of mild steel in HCl solution. Corrosion Science, 52:152-160.
32. Durnie W, Marco RD, Jefferson A, Kinsella B, 1999. Development of a structure-activity relationship for oil field corrosion inhibitors. Journal of Electrochemical Society, 146:1751-1756.
33. Martinez S, Stern I, 2002. Thermodynamic characterization of metal dissolution and inhibitor adsorption processes in the low carbon steel/mimosa tannin/sulfuric acid system. Applied Surface Science, 199:83-89.
34. Banerjee G, Malhotra SN, 1992. Contribution to adsorption of aromatic amines on mild steel surface from HCl solutions by impedance, UV, and Raman spectroscopy. Corrosion, 48:10-15.
35. Amin MA, Abd El-Rehim SS, El-Sherbini EEF, Bayyomi RS, 2007. The inhibition of low carbon steel corrosion in hydrochloric acid solutions by succinic acid: Part I. Weight loss, polarization, EIS, PZC, EDX and SEM studies. Electrochimica Acta, 52:3588-3600.
36. Ec Hosary AA, Saleh RM, Shams El-Din AM, 1972. Corrosion inhibition by naturally occurring substances—I. The effect of *Hibiscus subdariffa* (karkade) extract on the dissolution of Al and Zn. Corrosion Science, 12:897-904.

37. Veloz MA, Gonzalez I, 2002. Electrochemical study of carbon steel corrosion in buffered acetic acid solutions with chlorides and $H_2S$. Electrochimica Acta, 48:135-144.
38. Sherif EM, Park SM, 2006. Effects of 1,4-naphthoquinone on aluminum corrosion in 0.50 M sodium chloride solutions. Electrochimica Acta, 51:1313-1321.
39. El-Sayed A, 1997. Phenothiazine as inhibitor of the corrosion of cadmium in acidic solutions. Journal of Applied Electrochemistry, 27:193-200.